The intracellular tyrosine residues of the ATP-gated $P2X_1$ ion channel are essential for its function

Emese Toth-Zsamboki[a,1], Cecile Oury[a,1], Hiroyuki Watanabe[b], Bernd Nilius[b], Jos Vermylen[a], Marc F. Hoylaerts[a,*]

[a] *Center for Molecular and Vascular Biology, University of Leuven, Herestraat 49, 3000 Leuven, Belgium*
[b] *Laboratory of Physiology, University of Leuven, Herestraat 49, 3000 Leuven, Belgium*

Received 22 May 2002; accepted 10 June 2002

First published online 2 July 2002

Edited by Maurice Montal

Abstract The four highly conserved intracellular tyrosine residues of the $P2X_1$ ion channel were mutated into phenylalanine. Simultaneous electrophysiological and calcium measurements in transfected human embryonic kidney (HEK 293) cells indicated that Y362F and Y370F mutants were non-functional, despite their proper plasma membrane expression. The Y16F and Y363F mutants retained 2.2% and 26% of the wild-type $P2X_1$ activity, respectively. However, no tyrosine phosphorylation was detected on Western blots of $P2X_1$ immunoprecipitates derived either from HEK 293 cell lysates or from human platelets, expressing $P2X_1$ endogenously. Thus, Y16, Y362, Y363 and Y370 are required for the appropriate three-dimensional structure and function of the intracellular $P2X_1$ domains. **© 2002 Federation of European Biochemical Societies. Published by Elsevier Science B.V. All rights reserved.**

Key words: $P2X_1$ receptor; ATP-gated non-selective cation channel; Tyrosine residue; Site-directed mutagenesis; Three-dimensional structure

1. Introduction

P2X receptors are ATP-gated cation channels constituting a subfamily of purinergic (P2) receptors comprising seven distinct members ($P2X_1$–$P2X_7$) [1]. They form homo- or hetero-oligomeric ion channels in numerous excitable and non-excitable cell types and regulate a broad range of physiological processes [2]. The $P2X_1$ receptor mediates rapidly desensitizing non-selective cation influx [3]; generation of $P2X_1$-null mice has demonstrated a crucial role for the receptor in normal male fertility [4], but contributions to human bladder function [5], to vascular smooth muscle tone regulation [6] and to platelet activation [7,8] have also been suggested.

P2X subunits contain intracellular N- and C-termini and two hydrophobic membrane-spanning segments separated by a huge, highly glycosylated extracellular loop [9]. Although the channel pore, allowing entry of Na^+, K^+ and also Ca^{2+} ions, is believed to be in the second transmembrane domain, other domains, including the first transmembrane domain and the intracellular N- and C-terminal regions, also strongly contribute to the complex multifactorial allosteric process of channel pore opening and closing [10]. Indeed, truncations, deletions and mutations in these regions greatly affect the kinetics, permeation and desensitization of P2X channels [11].

Phosphorylation of intracellular serine, threonine and tyrosine residues is an important mechanism to modulate short- and long-term activity of ion channels and cell surface receptors [12]. In the slowly desensitizing $P2X_7$ channel, phosphorylation of a single tyrosine residue at position 343 is required to maintain the run-down of the current as well as to sustain the interaction of $P2X_7$ with several, mainly cytoskeletal proteins [13]. In contrast, $P2X_2$ was reported not to be phosphorylated on tyrosines [13] although substitution of the conserved Y16 with cysteine leads to complete loss of ion channel function [14].

In this study, using site-directed mutagenesis, we found that substitution of any of the four highly conserved intracellular tyrosine residues with phenylalanine greatly reduces or abolishes the $P2X_1$ channel function. Phosphorylated tyrosines were not detected in $P2X_1$ immunoprecipitates from transfected human embryonic kidney (HEK 293) cells or human platelets. We conclude that intact intracellular tyrosine residues are required to generate the inward cation current upon $P2X_1$ stimulation and propose that they assure the integrity of the three-dimensional organization of the $P2X_1$ subunits.

2. Materials and methods

2.1. Cell culture and transfections

HEK 293 cells [15] were transfected using the FuGENE 6 transfection reagent (Roche Diagnostics) according to the instructions of the manufacturer.

2.2. Expression vectors and mutagenesis of the human $P2X_1$ receptor

Site-directed mutagenesis was performed by the overlap primer extension method [16]. The previously described pcDNA3-$P2X_1$ expression vector [15] was taken as the template for PCR (Taq polymerase, Gibco). The following overlapping primers were used: Y16F: 5′-CATGCGGGGGGTGTCAAACTCG-3′, 5′-GCCTTCCTCTTCGAGTTTGACA-3′; Y362F: 5′-CTTCTTCTGCTTGTAGAAGTGC-3′, 5′-CTGCCTAAGAGGCACTTCTACA-3′; Y363F: 5′-GAACTTCTTCTGCTTGAAGTAG-3′, 5′-GCCTAAGAGGCACTACTTCAAGC-3′; Y370F: 5′-CCCATGTCCTCAGCGAATTTG-3′, 5′-CAGAAGAAGTTCAAATTCGCT-3′, together with primers specific for the pcDNA3 SP6- and T7-promoter sequences: SP6: 5′-GCATTTAGGTGACACTATAGAATAG-3′, T7: 5′-TAATACGACTCACTATAGGG-3′. Y16F, Y362F, Y363F and Y370F pcDNA3 and pcI-neo-IRES-GFP [17] expression vectors were produced. Oligonucleotide primers were designed to introduce the FLAG epitope (DYKDDDDK) into the carboxyl-termini of the $P2X_1$ wild type, immediately upstream of the stop codon: 5′-CCAGACCTCGAGCGGCCTCAT-

*Corresponding author. Fax: (32)-16-345990.
E-mail address: marc.hoylaerts@med.kuleuven.ac.be (M.F. Hoylaerts).

[1] These authors contributed equally to this article.

0014-5793/02/$22.00 © 2002 Federation of European Biochemical Societies. Published by Elsevier Science B.V. All rights reserved.
PII: S0014-5793(02)02987-3

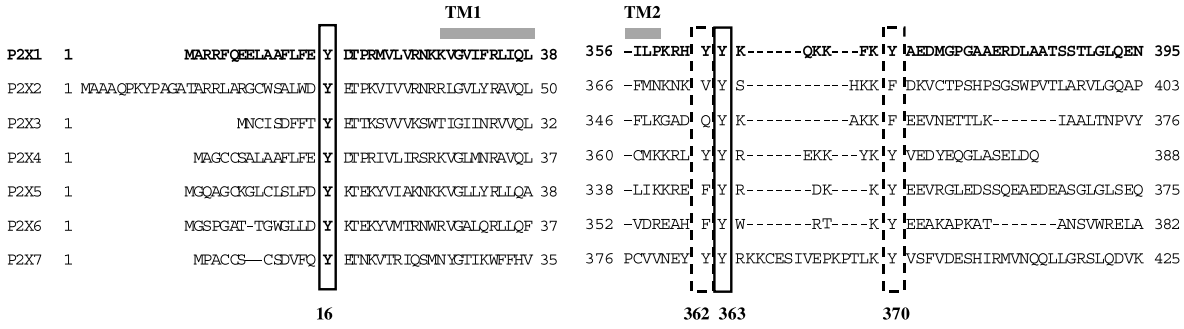

Fig. 1. Sequence alignment of human P2X receptors. Conserved tyrosine residues are boxed with solid lines and partially conserved residues with dashed lines. $P2X_1$ transmembrane domains (TM1 and TM2) are overlined with a bar. GI accession numbers are: 1709519, 12643353, 3024336, 2499422, 12643425, 3914240, 3915804 for the human $P2X_1$–$P2X_7$, respectively.

CAGG-3′, 5′-CCCTCTAGATTACTTGTCATCGTCATCCTTGTAGTCGGATGTCCTCATGTTCTCCTG-3′. All constructs were verified by sequencing (AutoRead Sequencing kit, Pharmacia Biotech).

2.3. Immunostaining and confocal microscopy

Immunofluorescent staining and confocal microscopy of HEK 293 cells grown on polylysine-coated culture slides were performed as described, using 25 μg/ml polyclonal rabbit anti-$P2X_1$ antibodies [15].

2.4. Electrophysiological recordings

$P2X_1$ function was analyzed 36–72 h after transfection with the bicistronic pcI-neo-IRES-GFP expression vector, using the whole-cell patch clamp method as previously described [15]. Briefly, the standard external bath solution contained 150 mM NaCl, 6 mM CsCl, 1 mM $MgCl_2$, 1.5 mM $CaCl_2$, 10 mM HEPES, 10 mM glucose, 50 mM mannitol (pH 7.4). The patch pipet solution contained 40 mM CsCl, 100 mM aspartic acid, 1 mM $MgCl_2$, 10 mM HEPES, 5 mM EGTA, 1.928 mM $CaCl_2$ at pH 7.2 to adjust the free $[Ca^{2+}]_i$ to 100 nM which suppresses activation of the endogenous Ca^{2+}-activated Cl^- channels in HEK 293 cells (Ca-buffer program; G. Droogmans, ftp://ftp.cc.kuleuven.ac.be/pub/droogmans/cabuf.zip). ATP (100 μM, Sigma) was applied for 10 s, at −80 mV holding potential. Data were sampled at 5 ms, filtered at 3 kHz; statistical comparison was made using the non-paired Student *t*-test.

2.5. Intracellular calcium concentration measurement

Cells were loaded with fura-2 (K^+ salt, 100 μM) included in the internal solution (40 mM CsCl, 100 mM aspartic acid, 1 mM $MgCl_2$, 10 mM HEPES and 0.1 mM EGTA) and applied through the pipet. Excitation wavelengths were alternatively 360 and 390 nm; fluorescence was measured at 510 nm. Apparent free Ca^{2+} concentration was calculated after subtraction of autofluorescence, from the fluorescence ratio R: $[Ca^{2+}]_i = K_{eff}(R-R_0)/(R_1-R)$ (K_{eff}, effective binding constant; R_0, fluorescence ratio at zero calcium concentration; R_1, fluorescence ratio at high Ca^{2+} concentration) [18]. For simultaneous measurements of membrane current and $[Ca^{2+}]_i$, currents were monitored in voltage clamp mode with an EPC-9 amplifier (HEKA Elektronik, Lambrecht, Germany, sampling rate 1 ms, 8-pole Bessel filter 2.9 kHz).

2.6. Immunoprecipitation and Western blotting of $P2X_1$ proteins

HEK 293 cells expressing the FLAG-tagged $P2X_1$ were lysed in ice-cold 1% Triton X-100 buffer (50 mM Tris–HCl, pH 7.4, 150 mM NaCl, 1 mM EDTA, 1% Triton X-100) containing 1/25 diluted protease inhibitor cocktail tablets (Boehringer, Mannheim, Germany), 25

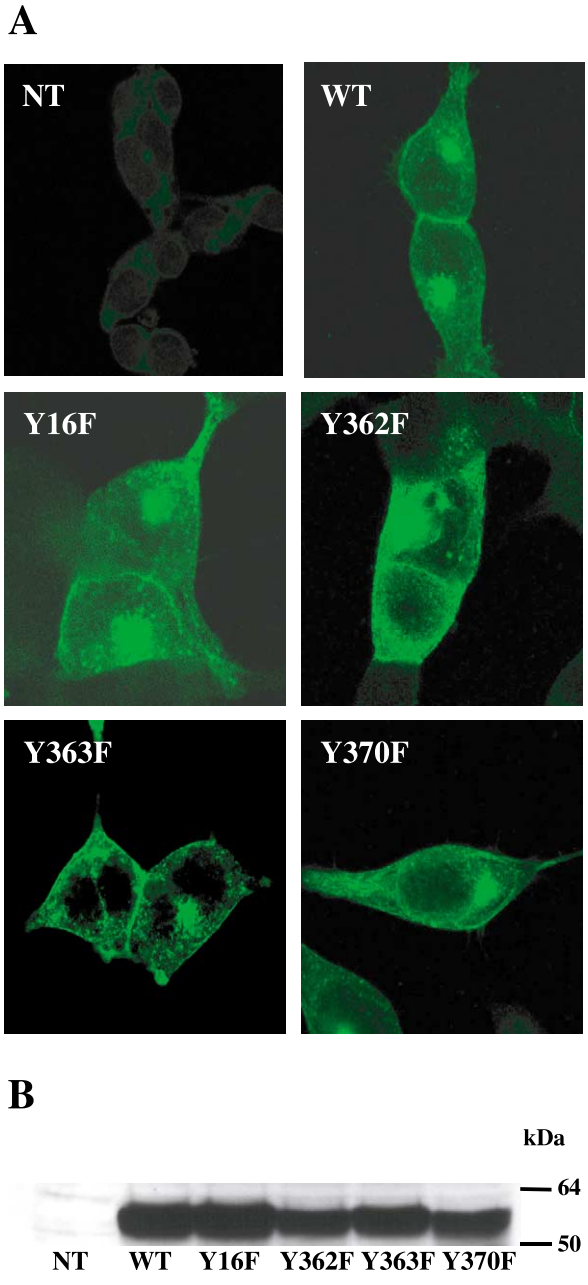

→

Fig. 2. Normal membrane localization and expression level of mutant $P2X_1$ channels. A: Confocal microscopy, following immunostaining of the wt and the four mutant $P2X_1$ channels in stably transfected HEK 293 cells. Non-transfected (NT) cells are shown as negative controls. B: Western blots of wt and mutant $P2X_1$-expressing HEK 293 cell extracts (same batch of cells used for electrophysiological measurements).

mM sodium fluoride and 1 mM sodium vanadate. When indicated, cells were pretreated with a selective, non-hydrolyzable agonist, α,β-methyleneATP (α,β-meATP, 100 μM, Sigma) for 1 min, with 1 U/ml apyrase (Grade I, Sigma) for 45 min or with 100 μM $NaVO_3$ for 30 min prior to extraction. Immunoprecipitation was performed by adding equilibrated anti-FLAG M2 affinity gel (Sigma) according to the protocol provided by the manufacturer. Proteins were separated on 12.5% SDS–polyacrylamide gel and were transferred to nitrocellulose membranes. Phosphorylated tyrosines were detected with a murine monoclonal horseradish peroxidase (HRP)-conjugated anti-phosphotyrosine antibody (HRP-4G10 clone, Campro Scientific). After stripping, total $P2X_1$ proteins were revealed by the home-made biotinylated rabbit anti-$P2X_1$ antibody [19] using the ABComplex (Dako). The same antibody was used for direct Western blotting detection of $P2X_1$ mutant proteins. Protein bands were visualized with an ECL kit (Amersham Pharmacia).

2.7. Preparation of washed human platelets and shape change analysis

Fresh blood obtained from healthy donors was anti-coagulated with acid–citrate–dextrose pH 6.2 (ACD) and centrifuged at $150\times g$ for 15 min in the presence of 1 U/ml apyrase. Platelet-rich plasma was diluted three-fold with ACD before centrifugation at $800\times g$ for 10 min. Platelets were resuspended at 2.5×10^5 platelets/μl in Tyrode's buffer (137 mM NaCl, 12 mM $NaHCO_3$, 2 mM KCl, 0.34 mM Na_2HPO_4, 5.5 mM glucose, 1 mM $MgCl_2$ and 5 mM HEPES, pH 7.3) containing 2 U/ml apyrase. The apyrase treatment, by degrading nucleotides released during platelet preparation, is required to maintain $P2X_1$ functionality [7]. $P2X_1$-mediated platelet shape change was recorded as a decrease in light transmission on an ELVI 840 aggregometer.

2.8. Immunoprecipitation of the $P2X_1$ receptor from human platelets

900 μl aliquots of washed human platelets were lysed with 10× concentrated ice-cold buffer containing protease and phosphatase inhibitors (see Section 2.6). When indicated, platelets were preincubated with 100 μM $NaVO_3$, stimulated with 2.5 μM α,β-meATP or with 1 μg/ml collagen (collagen reagent horm, Nycomed). Immunoprecipitation was performed using 25 μg/ml of a home-made rabbit anti-$P2X_1$-FLAG antibody and 50 μl of protein G beads (Santa Cruz). This antibody was raised against the native $P2X_1$-FLAG protein expressed in HEK 293 cells. After overnight incubation at 4°C, proteins were eluted with SDS buffer and were separated by 12.5% SDS–PAGE. Detection of the $P2X_1$ protein and the phosphotyrosine residues was performed as above (see Section 2.6)

3. Results and discussion

3.1. Normal membrane localization and expression level of the mutated $P2X_1$ channels

Sequence alignment of the rat, mouse and human $P2X_1$ indicates that the intracellular tyrosine residues in the N- and C-termini are conserved among different species. Moreover, intracellular tyrosines are completely (Y16, Y363) or partially (Y362, Y370) conserved within the human P2X ion channel family (Fig. 1). We mutated these residues into phenylalanine, generating four mutants (Y16F, Y362F, Y363F, Y370F). Immunostaining of wild-type (wt) and mutant $P2X_1$-transfected HEK 293 cells revealed similar expression, overall subcellular distribution and proper plasma membrane localization (Fig. 2A). Western blot analyses also indicated identical total $P2X_1$ protein levels (Fig. 2B).

3.2. Mutant $P2X_1$ subunits form non-functional or incapacitated channels

The $P2X_1$ channel mediates a rapidly desensitizing fast inward cation current, coinciding with an explicit intracellular calcium increase [2]. Saturating concentrations of ATP (100

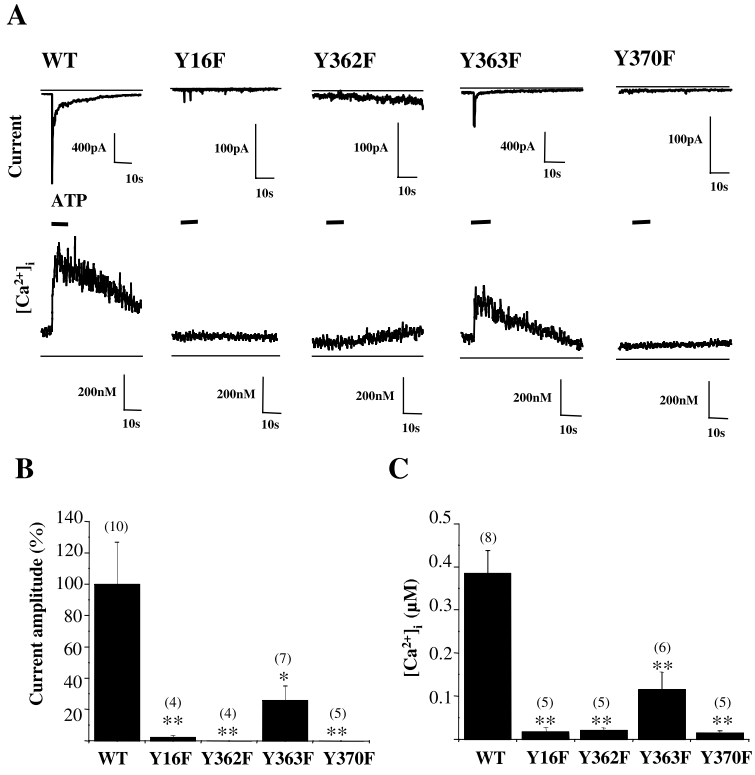

Fig. 3. $P2X_1$ channel activity in transfected HEK 293 cells. A: Representative examples of ATP-induced inward currents and parallel intracellular calcium measurements in wt and Y16F, Y362F, Y363F, Y370F $P2X_1$-expressing cells. Agonist application is depicted by bars. – = level of zero current or zero calcium concentration. Note the different current scale for the inactive mutants. B: Summary of the ATP-induced mean peak current recorded during the separate electrophysiological measurements. C: Main peak intracellular calcium increase in HEK 293 cells transfected with mutant cDNAs. Values are expressed as a percentage of the wt channel activity. (*$P<0.005$, **$P<0.001$.)

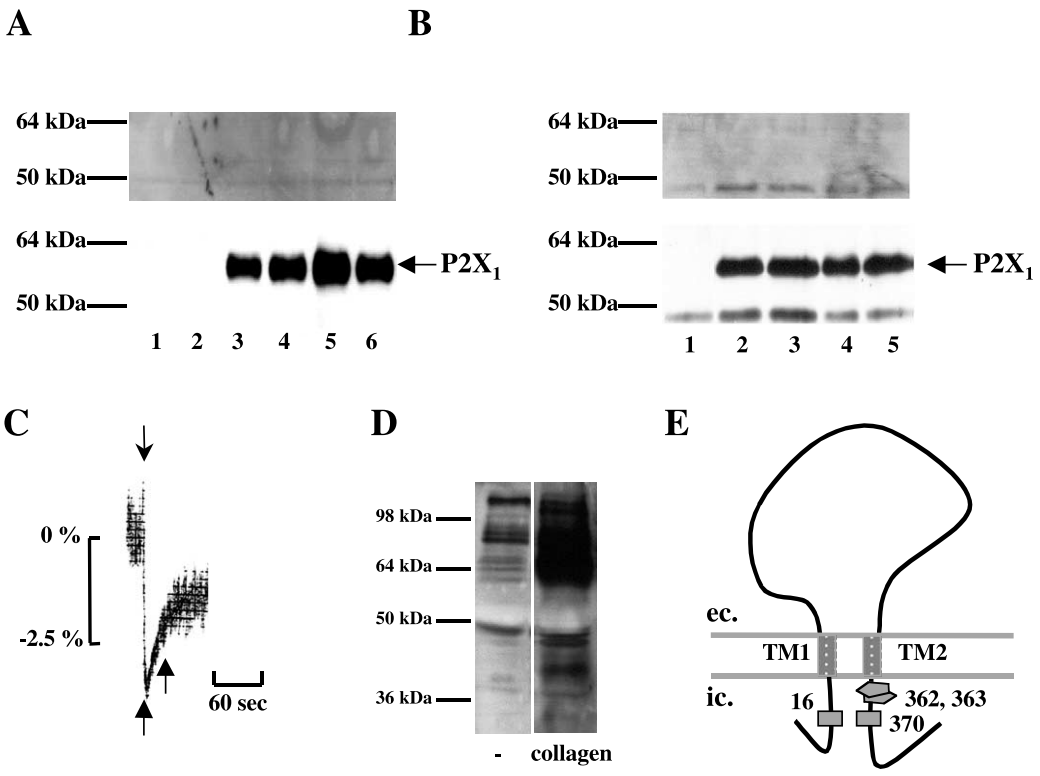

Fig. 4. Lack of tyrosine phosphorylation of the $P2X_1$ protein. A: Western blot detection of wt $P2X_1$-FLAG proteins immunoprecipitated from transfected HEK 293 cell extracts using an anti-phosphotyrosine 4G10-HRP-conjugated antibody (upper panel) or a polyclonal anti-$P2X_1$ antibody (lower panel). Lanes are: immunoprecipitation without cell lysate (1), non-transfected cells (2), wt transfected cells (3), wt cells treated with apyrase (4) and with $NaVO_3$ (5), or stimulated with α,β-meATP (6). B: Western blot detection of phosphorylated (upper panel) and total (lower panel) $P2X_1$ proteins immunoprecipitated from human platelets. Lanes are: immunoprecipitation without platelet lysate (1), resting (2), resting, $NaVO_3$-treated platelets (3), platelets stimulated with α,β-meATP for 5 (4) and 30 (5) s. C: Shape change induced by 2.5 μM α,β-meATP in human washed platelets. Lower arrows indicate the time of protein extraction, upper arrow represents the agonist application. Scales are light transmission and time, respectively. D: Tyrosine phosphorylation of platelet cytoskeletal proteins before and after stimulation with collagen (1 μg/ml, 5 min) using the same anti-phosphotyrosine antibody as in (A) and (B). E: Schematic representation of the $P2X_1$ subunit structure and intracellular tyrosines. The opposite orientation of Y363 to Y362 is indicated by arrow symbols.

μM) induced a robust inward current and an accompanying intracellular calcium increase in all wt transfected cells (mean peak current ± S.E.M. = 0.7191 ± 0.193 nA/pF, $n = 10$; mean peak calcium increase ± S.E.M. = 0.3852 ± 0.0538 μM, $n = 8$) (Fig. 3A). The Y362F and Y370F mutants were non-functional (no current, $n = 4$ and 5, respectively) and unable to trigger intracellular calcium influx (mean peak increase ± S.E.M. = 0.0206 ± 0.006 and 0.0146 ± 0.005 μM, respectively, $n = 5$ for both mutants, $P < 0.001$). The Y16F mutant retained 2.2% of wt channel activity (mean peak current ± S.E.M. = 0.023 ± 0.015 nA/pF, $n = 4$, $P < 0.001$), detectable only by high-sensitivity patch clamp measurements. Finally, the Y363F mutant was 26% active (mean peak current ± S.E.M. = 0.105 ± 0.0376 nA/pF, $n = 7$, $P < 0.005$ and mean peak calcium increase ± S.E.M. = 0.1155 ± 0.041 μM, $n = 6$, $P < 0.001$) (Fig. 3A). The Y16F and Y362F mutants had a rapidly desensitizing phenotype similar to that of the wt $P2X_1$. Non-transfected cells did not generate ion currents in response to ATP, but 15% of the cells produced a slow, delayed calcium increase in the absence of ion influx after ATP application. This can be explained by the fact that some HEK 293 cell lines express endogenous P2 receptors belonging to the metabotropic P2Y family [19]. Therefore, to calculate ATP-induced calcium increases, we used only those cells where the increase of Ca^{2+} coincided with the fast inward current.

These results indicate that substitution of tyrosines at positions 362 and 370 abolishes channel activity, while substitution of Y16 and Y363 drastically reduces it, showing the requirement of these residues for $P2X_1$ channel function (Fig. 3B,C). Generation of ion movement through the channel pore is a complex, delicate process, requiring several consecutive critical events. Since the ATP-binding site of P2X channels is located extracellularly [14], the most plausible explanation for the observed loss of activity would rely either on the impaired ability of the channel to open when ATP is bound, reflecting a decreased gating ability, or on reduced permeation, leading to loss of the current through the open channel.

3.3. *Lack of tyrosine phosphorylation of the heterologously expressed and endogenous $P2X_1$ proteins*

Phosphorylation of intracellular tyrosines provides control of receptor function, signaling events and assembly of multiprotein complexes. To assess whether the loss of ion channel activity is due to deficient tyrosine phosphorylation, we have searched for phosphorylated tyrosine residues in the wt $P2X_1$. Since the C-terminal FLAG sequence does not affect the properties of the $P2X_1$ channel [20], we transfected HEK 293 cells with a FLAG-tagged $P2X_1$ pcDNA3 expression vector to facilitate the immunoprecipitation procedure. Cells were treated with apyrase prior to extraction, to prevent receptor desensitization via breakdown of the spontaneously released nucleotides in cell culture media [21]. Cells were

also preincubated with the phosphatase inhibitor $NaVO_3$ or with the non-hydrolyzable $P2X_1$ agonist α,β-meATP. Repetitive Western blotting experiments failed to reveal phosphorylated tyrosines in the wt $P2X_1$ in any of these conditions (Fig. 4A).

Human platelets exclusively express the $P2X_1$ ion channel responsible for rapid, reversible calcium influx leading to platelet shape change [7]. Therefore, we used washed human platelets as native, $P2X_1$-expressing cells for immunoprecipitation; platelet shape change was analyzed in parallel to document preservation of $P2X_1$ functionality. We found no evidence of tyrosine phosphorylation in resting, in $NaVO_3$-treated or in α,β-meATP-stimulated platelets (Fig. 4B), even though the receptor was functional at the time of protein extraction (Fig. 4C). On the contrary, the collagen-induced tyrosine phosphorylation of numerous platelet cytoskeletal proteins [22] was clearly detected using the HRP-conjugated anti-phosphotyrosine antibody, as expected (Fig. 4D).

Our data indicate that all four $P2X_1$ tyrosine residues are required for an appropriate cation influx through the channel. Since no tyrosine phosphorylation can be detected in heterologously or endogenously expressed $P2X_1$ protein and the mutagenesis of either of the two adjacent residues (Y362 and Y363) leads to loss of function, the role of intracellular tyrosines in $P2X_1$ appears to be structural.

Since $P2X_1$ channels are thought to be composed of at least three homo-oligomers [1], 12 intracellular tyrosine residues are expected for each channel. Although the three-dimensional structure of the P2X-type ion channels is unknown, the N- and C-terminal tails are thought to be close to each other, sitting underneath the channel in a closed state (Fig. 4E) [2]. We speculate that the intracellular tyrosine residues contribute to a well-defined structure, localized just beneath the channel pore region. Tyrosine hydroxyl groups, by creating intramolecular hydrogen bounds, are important for protein folding [23] and contribute to protein stability [24]. It would therefore be interesting to determine whether similar structure–function relations exist in other P2X members. The most likely candidate for such a study would be the $P2X_4$ receptor, containing tyrosine-rich, short intracellular regions, highly homologous to those of $P2X_1$.

In conclusion, we report that intact intracellular tyrosine residues are essential to maintain the functionality of the rapidly desensitizing ATP-activated $P2X_1$ ion channel.

Acknowledgements: C.O. is holder of a postdoctoral research fellowship of the FWO. E.T.-Z. is the beneficiary of a KU-Leuven doctoral scholarship. Financial support was obtained from the FWO G.0376.01 project and from the Bilateral Scientific Cooperation Between Flanders and Hungary (BIL0012).

References

[1] Ravelic, V. and Burnstock, G. (1998) Pharmacol. Rev. 50, 413–492.
[2] Khakh, B.S. and Humphrey, P.P.A. (2001) Pharmacol. Rev. 53, 107–118.
[3] Evans, R.J., Lewis, C., Buell, S., Valera, S., North, R.A. and Surprenant, A. (1995) Mol. Pharmacol. 48, 178–183.
[4] Mulryan, K., Gitterman, D.P., Lewis, C.J., Vial, C., Leckie, B.J., Cobb, A.L., Brown, J.E., Conley, E.C., Buell, G., Pritchard, C.A. and Evans, R.J. (2000) Nature 403, 86–89.
[5] Vial, C. and Evans, R.J. (2000) Br. J. Pharmacol. 131, 1489–1495.
[6] Boarder, M.P. and Hourani, S.M.O. (1998) Trends Pharmacol. Sci. 19, 99–107.
[7] Rolf, M.G., Brearly, C.A. and Mahaut-Smith, M.P. (2001) Thromb. Haemost. 85, 303–308.
[8] Oury, C., Toth-Zsamboki, E., Thys, C., Tytgat, J., Vermylen, J. and Hoylaerts, M.F. (2001) Thromb. Haemost. 86, 1264–1271.
[9] Khakh, B. (2001) Nat. Rev. Neurosci. 2, 165–174.
[10] Jiang, L.H., Rassendren, F., Spelta, V., Surprenant, A. and North, R.A. (2001) J. Biol. Chem. 276, 14902–14908.
[11] Robertson, S.J., Ennion, S.J., Evans, R.J. and Edwards, F.A. (2001) Curr. Opin. Neurobiol. 11, 378–386.
[12] Yaffe, M.B. (2002) Nat. Rev. Mol. Cell. Biol. 3, 177–186.
[13] Kim, M., Jiang, L.H., Wilson, H.L., North, R.A. and Surprenant, A. (2001) EMBO J. 20, 6347–6358.
[14] Jiang, L.H., Rassendren, F., Spelta, V., Surprenant, A. and North, R.A. (2001) J. Biol. Chem. 276, 14902–14908.
[15] Oury, C., Toth-Zsamboki, E., Van Geet, C., Thys, C., Wei, L., Nilius, B., Vermylen, J. and Hoylaerts, M.F. (2000) J. Biol. Chem. 275, 22611–22614.
[16] Ausubel, F.M., Brent, R., Kingston, R.E., Moore, D.D., Siedman, J.G., Smith, J.A. and Stuhl, K. (1995) Mutagenesis of Cloned DNA. Current Protocols in Molecular Biology, pp. 8.5.1–8.5.7, Wiley, New York.
[17] Trouet, D., Nilius, B., Voets, T., Droogmans, G. and Eggermont, J. (1997) Pflug. Arch. Eur. J. Physiol. 434, 632–638.
[18] Nilius, B., Schwartz, G., Oike, M. and Droogmans, G. (1993) Pflug. Arch. Eur. J. Physiol. 424, 285–293.
[19] Schachter, J.B., Sromek, S.M., Nicholas, R.A. and Harden, T.K. (1997) Neuropharmacology 36, 1181–1187.
[20] Torres, G.E., Egan, T.M. and Voigt, M.M. (1999) J. Biol. Chem. 274, 6653–6659.
[21] Buell, G., Michel, A.D., Lewis, C., Collo, G., Humphrey, P.P.A. and Surprenant, A. (1996) Blood 87, 2659–2664.
[22] Bachelot, C., Cano, E., Grelac, F., Saleun, S., Druker, B.J., Levy-Toledano, S., Fisher, S. and Rendu, F. (1992) Biochem. J. 284, 923–928.
[23] Hamill, S.J., Cota, E., Chothia, C. and Clarke, J. (2000) J. Mol. Biol. 295, 641–649.
[24] Pace, C.N., Horn, G., Hebert, E.J., Bechert, J., Shaw, K., Urbanikova, L., Scholtz, J.M. and Sevcik, J. (2001) J. Mol. Biol. 312, 393–404.